Powder Technology 301 (2016) 141–152

Contents lists available at ScienceDirect

Powder Technology

journal homepage: www.elsevier.com/locate/powtec

Visualization system for the measurement of size and sphericity of char particles under combustion conditions

Wojciech P. Adamczyk [a,*], Andrzej Szlęk [a], Adam Klimanek [a], Ryszard A. Białecki [a], Gabriel Węcel [a], Anna Katelbach-Wozniak [a], Slawomir Sładek [a], Mario Ditaranto [b], Nils Erland L. Haugen [b]

[a] Institute of Thermal Technology, Silesian University of Technology, Gliwice, Poland

[b] SINTEF Energi A.S., Sem Saelands vei 11, 7034 Trondheim, Norway

ARTICLE INFO

Article history:
Received 29 December 2015
Received in revised form 24 May 2016
Accepted 2 June 2016
Available online 4 June 2016

Keywords:
Tracking particles
Visualization system
Particle size
Kinetic

ABSTRACT

Advanced visualization systems are used in many engineering applications where information about particle size and position plays critical roles. In practice, the manual detection and following of individual or groups of particles is not feasible; an automated computational method must be used. Devices and mathematical algorithms capable of tracking particles have been developed by many engineering groups. The applicability of available methods is limited to detecting and tracking particle size and position only under cold flow conditions being the main weakness of these methods. To mitigate this limitation, a unique experimental rig and detection algorithm used for calculating particle size and sphericity under combustion process are investigated in this study. The data collected by the proposed visualization system are used to gather kinetic data of combustion. Reliable kinetic data are critical for accurate simulations of coal combusted in the large industrial boilers used in the energy sector, and thus, they are a pre-requisite for computer aided boiler optimization.

1. Introduction

Within the energy sector, where fossil fuels are commonly used, there is a question on how the fuel conversion process can be improved in order to reduce cost while keeping the pollutant emission within admissible range. The answer for this question can be given by application of the complex numerical models based on the Computational Fluid Dynamics (CFD). An example of such application can be found in works [1,2] and [3,4] where the advanced numerical techniques were used for modeling combustion process in experimental rig and large scale pulverized coal (PC) boilers. A necessary condition to achieve simulation accurate results is the access to appropriate kinetic data for the burned fuel. These data can be obtained only experimentally using dedicated devices.

Combustion of a coal particle undergoes in several steps. When the solid particle is exposed to hot gases (i.e., combustion products), the particle mass can change due to three processes: moisture evaporation, devolatilization (i.e., pyrolysis) and char combustion [5]. Depending on the particle size, those three processes can occur sequentially (large particle) or simultaneously (small particle). Evaporation under industrial conditions takes place within the coal mills where coal or biomass is heated to the desired temperature by hot primary air or recirculated flue gases. This stage is required to avoid blocking of the primary pipe which supplies pulverized coal to the burners. Contact of the particle with gas phase temperature of above 300 °C volatile matter consisting of light gases, tar, and remaining water is released. This stage is strongly connected with heating rate, composition of the gas and pressure [6]. The characteristic feature of devolatilization is that the gases which diffuse to the particle surface can cause its swelling. Bituminous coals [7,8] undergo such process, lignite particles may fragment [9]. The last step of coal combustion is the char oxidation, which is the slowest step of the overall coal combustion process. The rate of coal combustion process is related to its composition and structure as well as the composition, pressure and temperature of the oxidizer. The coal burning rate in turn affects residence time of the particles in combustion chamber and therefore influences the overall heat transfer processes and efficiency of the combustion process. Char oxidation is controlled by two processes: diffusion and kinetics (chemical control) [10]. At high temperatures, the rate is controlled by diffusion, while at low temperatures, the rate is controlled by chemical kinetic. However, under certain conditions, chemical reactions can proceed simultaneously either on the particle surface (diffusion) or within the particle (kinetic). As char combustion rate directly influences on the amount of unburned carbon (UBC), which affect plant thermal efficiency, it is very important to use reliable submodels of combustion rate to be embedded in the overall model of the boiler.

To determine the kinetic data of a given type of coal, several parameters must be known, including particle dimension, shape, rate of the particle mass loss and particle surface temperature [11,12]. The last

* Corresponding author.
E-mail address: wojciech.adamczyk@polsl.pl (W.P. Adamczyk).

http://dx.doi.org/10.1016/j.powtec.2016.06.004
0032-5910/

parameter is difficult to measure [13,14]. These parameters are often used as the input for CFD models of combustion processes of industrial Pulverized Coal (PC) and Circulating Fluidized Bed (CFB) boilers to predict concentration of NOx and CO, temperature and flow field throughout the boiler. Coal kinetics data are then used to calculate the temporal mass variation of particles using mathematical formulae containing many coefficients [11,15]. The values of the latter are obtained by fitting them with experimental data. The most popular methods to acquire experimental data are Drop Tube Furnaces (DTF) [16,17,18] and Thermogravimetric analysis (TGA) [19,10,20]. Over the years, the DT reactor becomes experimental technique of choice for determining both combustion rates of volatile matter and char in various operating conditions. The strength of this technique is the heating rates up to 10,000 K/s which are similar to those expected within the real pulverized boilers. Fig. 1 (left) illustrates the design of DTF. The general measurement idea is as follows. The coal particles are injected to the reactor at its upper part and they are carried by the gases through the reactor. To ensure isothermal conditions the temperature of the external walls of the DTF is controlled by electrical heaters. Depending on the position of the collector the residence time of the particles can change which ensures different combustion rates of the particles. The composition of the oxidant (flue gases) is controlled by the excess air used in the combustion process of the hydrocarbon fuel, typically methane. The set of experiments is always run for several temperatures, particle residence times, and oxidation atmospheres, collected by the sample collector and the solid separator is then analyzed using TGA to determine remaining fraction of combustible matter in particles. In the case of using DTF for measuring combustion rate of volatile matter, the measurement procedure is the same, except the oxidant that is replaced by an inert gas (nitrogen or helium) to prevent uncontrolled char ignition at high temperature. DTF provides accurate data, nevertheless the running of experiments is very expensive and requires experienced operating staff. Moreover, the collected samples need to be further analyzed using TGA to determine their UBC fraction.

The TGA allows to track the changes of the coal particles weight as the function of time and temperature [21,22]. It can be applied also for other materials like biomass, wastes, and sewage sludge. The scheme of TGA device is depicted in Fig. 1 (right). The sample of coal (typically 1 mg to 30 mg) is placed on the load cell in an enclosure with controlled oxidation atmosphere. The TGA can also be used for carrying out proximate analysis [23]. The advantage of TGA over DTF is relatively simple and cheap the measurement process. However, in real pulverized coal combustion process that occure within PC boilers the particles heating rate is much faster than 1 K/s which can be achieved in TGA. That is the main reason why the kinetic data received from TGA experiments cannot be directly used. Nevertheless, the kinetic data retrieved in chemically controlled regime **I** [15] using TGA at temperature range from 700 °C to 1050 °C can be further extended to kinetic/diffusion (**II**) and diffusion (**III**) zones using the kinetic/diffusion model [11,24]. To use this approach, the particle temperature, and oxygen fraction in the vicinity of the particle have to be known, which is in practice difficult to obtain.

Nowadays, many efforts are made to develop advanced vision system for characterization and analysis of the char combustion under various conditions. Vision systems give possibility to observe changing of the particle diameter, structure or propagation of ignition at relatively low cost [25]. Literature describes some application of vision system [26,27]. Both papers used a visualization system to trace a single particle under different atmospheres during combustion. In their studies, a visualization system was used to observe behaviour of the falling particles, where both the moment of ignition, and particle swelling or breakage processes were caught. Cloke et al. [28] applied the vision system for measuring particle porosity, size and wall thickness. In recent advanced studies [29,30] the Infrared Camera (IR) was used to record the particle temperature and changes of the particle size. The calculated intrinsic reaction rate constant for lignite coal based on the measured particle mass loss shows very good agreement with the experimental data measured using TGA device. Other application of the vision system for measuring

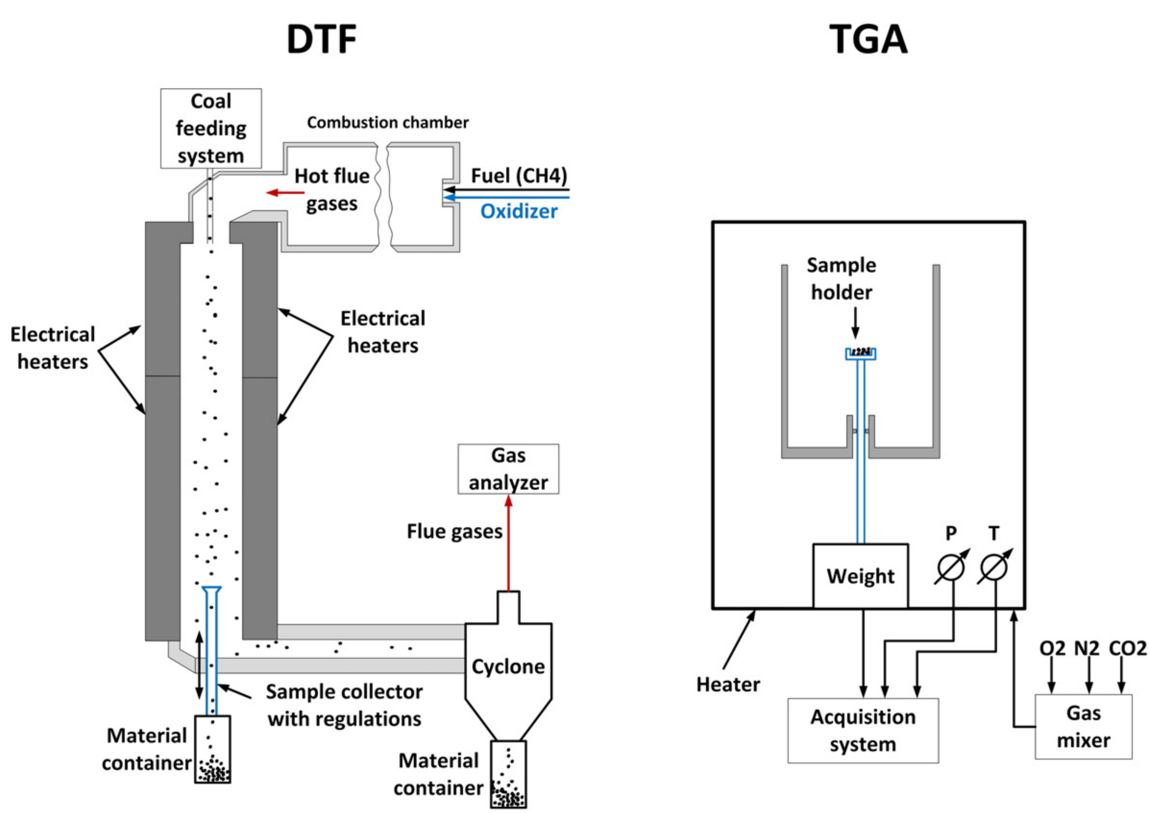

Fig. 1. Construction of the drop tube furnace (left) and thermogravimetric device (right).

particle diameter and temperature under fluidization process has been also reported in works [31,32]. Despite the wealth of the available vision systems there is still room for improvement. A good example of such activities is the application of vision system for tracking simultaneously a number of particles combined with advanced mathematical model for retrieving coal kinetic data based on inverse analysis [33].

To combine advantages of both the mentioned measurement methods, mainly the high heating rate of the DTF, possibility of tracking particle mass losses as of the DTF, recording the moment of particle ignition (TGA), together with the possibility of retrieving kinetic data in kinetics/diffusion controlled zone **II**, a new and unique experimental rig and advanced particle tracking software have been proposed in this study. The built rig provides the possibility to track a single particle at the micrometre scale (from 90 μm up to 220 μm), temperature range from 800 °C up to 1100 °C, and under different oxidizer mixtures $O_2/N_2/CO_2$. The device allows for capturing the particle ignition, exact combustion time, particle sphericity, and changes of particle diameter during combustion process. The visualization system collects particle trajectories which are then used in an inverse analysis to determine the rate of burned char. Combining the tracking application with inverse char kinetics data almost online in contrast to other methods which require lengthy and laborious procedures.

2. Methodology

The primary element of the rig, depicted in Fig. 3 is a thin horizontal heated slot with optical windows used to track the trajectories of the carried by the hot gases particles. Hot gas, which represents a combustion environment, flows horizontally through the slot. A pulverized char particle is then injected at the top of the slot through the ports located in the upstream gas flow. The particles leaving the ports begin to move downstream with the gas. After reaching terminal velocity, the particles move along a given trajectory that depends on the gas temperature, composition, char type and particle diameter. For an inert gas, the trajectory is a straight line. If the gas contains oxygen, and its temperature is sufficiently high to initiate combustion, the trajectory begins to flatten out. Due to combustion, the char particle loses mass, and thus, its vertical velocity component decreases. The trajectory of the char particle is observed through an optical window via a CMOS camera. The trajectories are recorded and stored for later processing.

The proposed experimental rig has been designed and built to observe the combustion process of both a single char particle and a group of char particles under conditions similar to those observed within industrial pulverized coal boilers. The primary idea of the procedure used for measuring the combustion kinetic data of a single coal particle is shown in Fig. 2. Under ideal conditions, the particle released into the flowing inert gas should achieve vertical and horizontal velocity components that are comparable to the gas velocity after short period of time. Note that without combustion, the particle diameter remains constant, and there is no mass loss. As a result, the particle carried by inert gas should drop at 45 ° to the horizontal plane. Under combustion conditions, when the mass and diameter of the char particle decreases over time, the falling trajectories begin to diverge from the straight trajectory. Finally, when all the char of a particle is consumed by the chemical reactions, the particle will only consist of ash. The last step of the particle combustion process is carrying it towards the outlet of the experimental rig.

Based on the information that the gravitational force, which depends on the particle mass, is in the vertical direction, while the aerodynamic drag that depends on particle diameter, acts both horizontally and vertically, the particle trajectory and changes in diameter can be used to determine the changes in particle mass over time. The recorded particle trajectories at every time instance are then used to determine the particle combustion rate by fitting them to the kinetic equation. An inverse procedure was applied to determine the kinetics data for which the simulated particle trajectory matches best the measured one. More information about formulated inverse problem will be given later.

The proposed measurement method provides relevant data which can be further applied for developing of the char combustion models used for mathematical modeling of the coal combustion process within industrial PC boilers. Nevertheless, before running the experiment the coal particles have to be appropriately prepared in order to ensure that only char combustion process will be observed. The as-received coal particles primarily consist of water, ash, volatile matter (VM), and char. Due to the construction of the rig the as-received particles cannot be directly used during experiments. Presence of water influences on the particle ignition, changes of the gas temperature in vicinity to the particles, and concentration of water vapor in gases can cause serious problems during rig operations. Moreover, the high fraction a VM within the coal particles, can led to its breakup into the number of smaller particles inducing problems with particle tracking. Some example of large particle brakeage process during coal devolatilization was described in [26]. Moreover, the gases released from particle causes fumigation of the observation window hindering the measurements. Within the first step of sample preparation the moisture associated with coal is evaporated. In the second step, the volatile matters are removed from the particles. This process was run at constant temperature (1000 °C) and in the inert gas atmosphere. In the next stage the dried and devolatilized coal particles are intensively milled to produce char particles below 220 μm. The last step is focused on sieving the char particle to ensure narrow range of the particle sizes injected in the experimental rig.

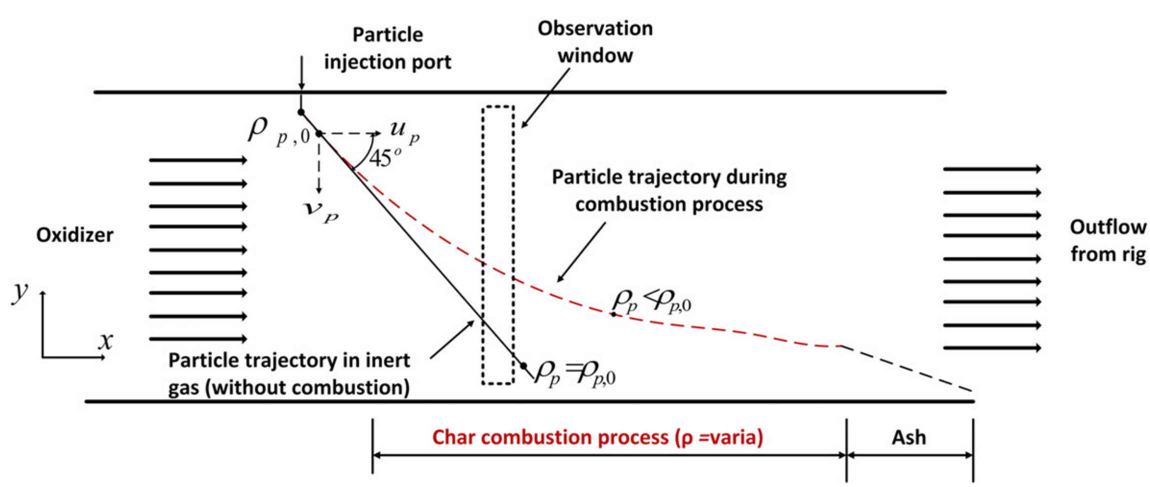

Fig. 2. Concept of the measurement procedure.

3. Experimental setup

The experimental setup used in this study to measure particle mass loss over time is shown in Fig. 3. The primary component of the test stand is the Electrical Heater (EH), which can heat the oxidizer/gas up to 1650 °C at maximum gas flow rate equal to 0.35 Nm ^{3}/h. The typical flow rates used during experiments in temperature range 900 °C to 1100 °C vary between 0.35 Nm ^{3}/h and 0.65 Nm ^{3}/h. The maximal gases velocity for developed velocity profile can reach up to 0.35 m/s depending on the oxidizer composition and temperature. The distance at which gas reaches the require temperature, which corresponds to size of the heater was checked numerically, where flow was calculated using the Ansys FLUENT [34] code. The three temperature profiles calculated along the heater, for oxidizer volumetric flow rate 0.63 Nm ^{3}/h and composition $O_2 = 15\%$ $CO_2 = 85\%$ are illustrated in Fig. 4. It can be seen that the electrical heater length equal to 0.800 m is sufficient to reach desired temperature at the EH outlet, for typical conditions maintained during measurement, see Fig. 3. Second question tested numerically was the development of velocity profile along the heater. It can be seen in Fig. 4 that almost after 0.3 m distance from the inlet to the EH, the gas velocity profiles stabilize. Based on the performed simulations, and both the gas temperature and velocity the size of the electrical heater has been selected.

The primary heater is connected to a set of electrical heaters, which helps to maintain the gas temperature at a constant level. The maximum heating temperature of each module cannot exceed 1100 °C. The cross-section of the gaseous slot in each heating section is 0.015 × 0.240 m, and the primary dimensions of the experimental setup are shown in Figs. 3 and 5. The heating temperature of each heater is controlled by the user through an external controller. The heating module with observation window is equipped with fuel feeding rail cooled by an external water circuit. At 0.025 m distance feeding rail has ports where the coal feeder can be mounted. The water cooling system prevents uncontrolled particle ignition in the channel and feeder. To ensure appropriate particle feed rate and particle dispersion, a custom coal feeding system has been designed. It consists of funnel, step motor, regulated screw, system for controlling step motor velocity and motor step division to ensure smooth particle feeding rate. To ensure stable gas flow through the rig during experiments, a special gas mixing system was designed. The system controls flows of two gases mixture O_2–N_2 or O_2–CO_2 using *Bronkhorst* flow controllers for regulating the flow in range from 0 Nm ^{3}/h to 2 Nm ^{3}/h.

The particle trajectories are observed and recorded by the visualization system through the optical window located on each side of the observation module. The cross-section through this module, in addition to a general view on the data acquisition system, is shown in Fig. 5. To prevent heat loses through the observation window, additional quartz barriers were placed in observation gap. To record the movable particle trajectories, a Vieworks VC-4MC-180 camera link equipped with a CMOS sensor and a maximum resolution of 2048 × 2048 was used.

Additional difficulties arose from the small field of view (FOV), which also created difficulties in selecting the appropriate lens system. Finally, for such conditions, a *ZEISS* lens *Apo Sonnar* with a high focal length (135 mm), and very small lens distortion (0.3%) was used. For this lens, the minimum focusing distance is 800 mm. From this distance at the highest resolution, the FOV is equal to 66 mm. In this study, the active FOV was reduced to one-quarter (1024 × 1024) of the total FOV because the observation field was equal to 25 × 25 mm, ensuring that the frame rate of the camera in the given configuration was equal to 183 Hz. One characteristic feature of the CMOS sensor used in this study is its high sensitivity to high temperature fluctuations. The camera was placed at a certain distance from the windows to protect it from the high temperature present in the experimental rig. To avoid camera damage, a hot mirror in the direction of the observation was also installed, which effectively screened the camera from infrared radiation. A hot mirror reflecting light at wavelengths above 750 μm was used because the monochrome camera operates in a spectral range from 380 to 850 μm. To track black particles carried by the inert gas (N_2), a LED backlight was used to ensure appropriate illumination during the recording of particle trajectories over a short exposure time. The backlight was installed at the opposite side of the observation module, which was also protected from heat damage by a hot mirror. When tracking burned particles, the backlight could be turned off because the burning particle would generate sufficient luminous intensity to be visible during short exposure times. Single-pixel intensity values could even attain values close to saturation at 254. This camera was installed on a traversing system to smoothly and accurately control its position and movements in three directions. The overall camera positioning system, the camera processes and the gas mixing system are all fully integrated through the in-house control application written in LabVIEW. To ensure a fast response, a portion of the control software has been written in real-time mode using FPGA processor. The application used for controlling hardware and software for tracking particles and calculating their diameters were written in LabVIEW. The used *state machine* technique in programmed applications gives the possibility to extend the capabilities of the applications in relatively easy way. The software will be described in the next section.

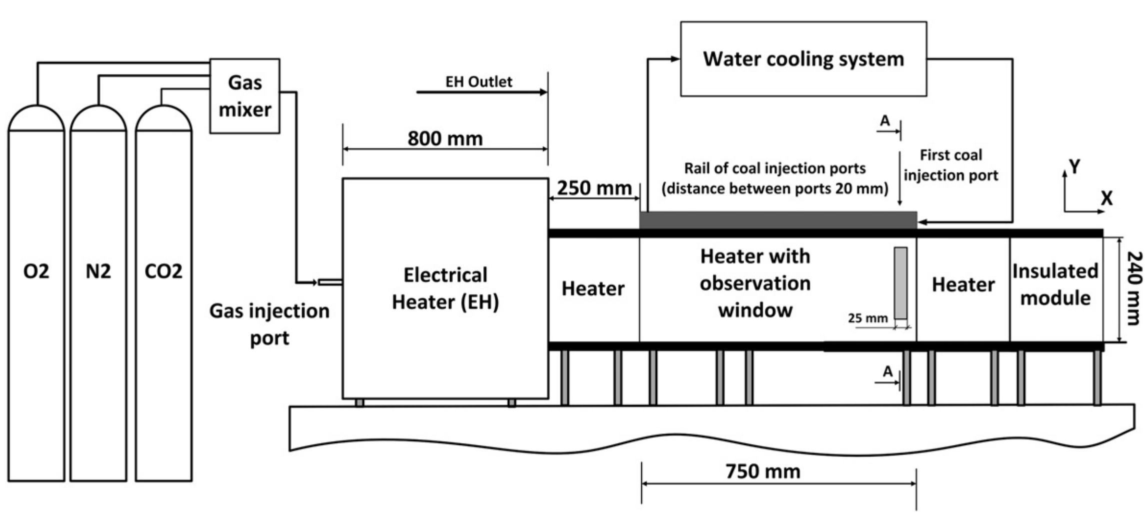

Fig. 3. Simplified drawing of the experimental rig.

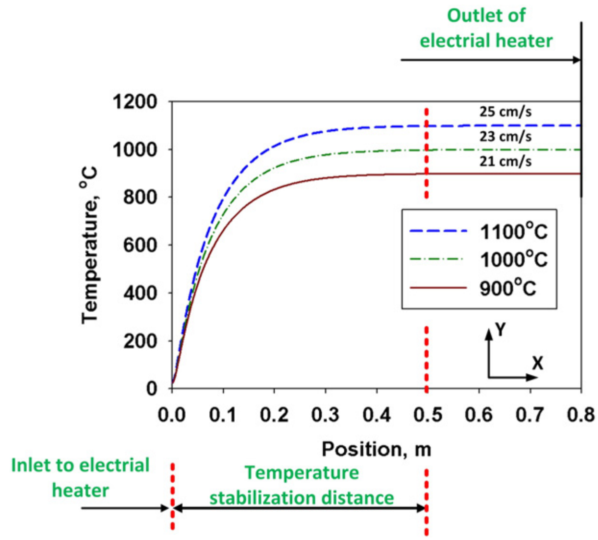

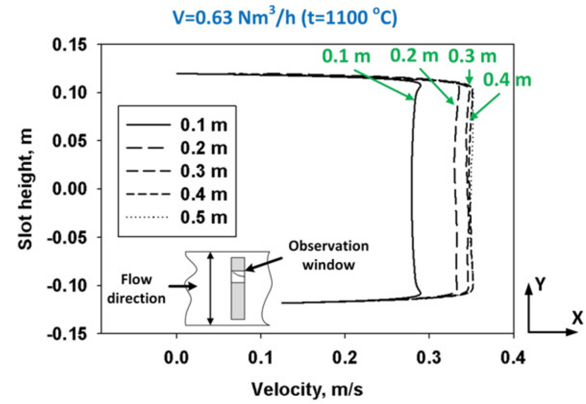

Fig. 4. Temperature (left) and velocity (right) profiles along the electrical heater.

4. Particle tracking procedure

The flow conditions within the rig have to be stabilized before starting the measurement campaign. Typically, such conditions are achieved after approximately four hours of heating. In order to minimize the consumption of the oxidizer, it is replaced by air at the heating stage. After switching from air to the required gas mixture, flow stabilization occurs within a few minutes.

Then, the coal feeder is activated, and the recording process can be started. The set of frames is recorded directly to an SSD mass storage to ensure high frame recording rate for given position of the camera, the number of recorded frames can reach 3000 depending on defined recording time. As illustrated in Fig. 3 the coal feeder can be placed at different positions, the pitch of the ports is equal to 20 mm. The total number of coal injection ports is equal to 30. The steps of measurement procedure are as follows: coal feeder is placed in the first injection ports, then the particles trajectories are recorded in the first upper position of the camera, after recording set of frames the camera is moved down of about 25 mm whereas the coal feeder is kept in the same position. The camera is moved sequentiality down until particles can be observed in given camera position. After these steppes the coal feeder is moved to next port and camera motion procedure is repeated. After completing the measurements, data are stored, and the tracking procedure can be activated in a post-processing mode.

Due to a too long time interval between subsequent frames (5.5 ms at 180 Hz), the standard procedure used in the Particle Image Velocimetry (PIV) technique cannot be applied, this is main reason that *in-house* tracking algorithm was developed. The standard PIV measurement technique requires seeding with many particles and enormous number of frames. Fig. 6 shows recorded frames by vision system, where some of the selected particles were tracked in four subsequent frames. Each of the particles was individually tracked by checking its position at the recorded frame where the time span between subsequent frames was 0.0055 s. The tracking procedure tracks particles as long as they appear in the subsequent recorded frame. In order to observe exactly the same particles dedicated procedure was implemented into the tracking algorithm.

In the proposed algorithm, the diameters of each detected particle in a given frame are calculated based on the pixel intensity (PI) values. Each of the pixel assume intensity value from 0 to 254; this value depends on the backlight power, whether the particle is burning or not, and the camera aperture position. For burning particles, the pixel intensities covered by the particle can reach the upper value, while for unburned particle, pixel intensities are closer to 0. For unburned particles (e.g., ash or particles tracked in inert gas), the developed tracking procedure works in the same way.

To track the burning particles, the procedure in the first step requires a definition of the threshold intensity range. The threshold range must

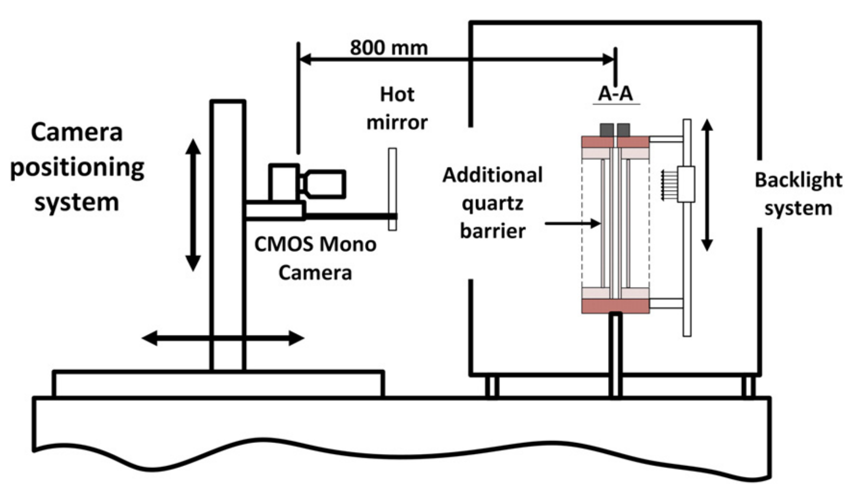

Fig. 5. Cross-section of the test rig and overview on the visualization system configuration.

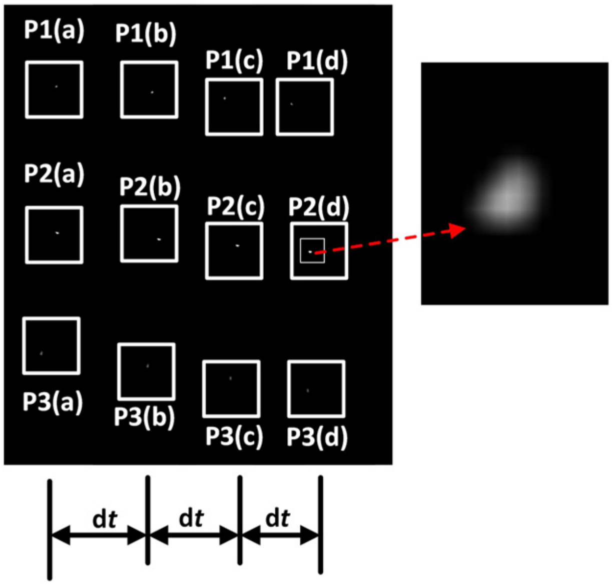

Fig. 6. Selected particles in subsequent recorded frames.

be appropriately defined for both the given oxidizer temperature and its composition. Pixels that have an intensity value in the defined range are recognized as the particle. As shown in Fig. 6, pixels that cover the tracked particle exhibit varying intensities, where the highest intensity can be observed at the centre of the particle. Due to the aspherical shape of the particle, this intensity does not proportionally attenuate itself out of the particle centre in each of the spatial directions. Due to the fact that the particle at the border can only cover part of the pixels, a special treatment is required to assume an intensity value lower than defined threshold range. A similar effect called the *Halo effect* has been described in the literature [35]. In the proposed setup, where the procedure is used to detect the size of the tracked particle, the influence of the pixel intensity at the detected particle border cannot be neglected.

The idea of the evaluation weights of the pixels intensities is shown in Fig. 7 (left). In the first step of the procedure, pixels that cover the detected particle and fit within the defined intensity range are used to calculate the average intensity value of the selected pixels (i.e., the Base Pixels Intensity, BPI). In the next step, a rectangular frame with a thickness equal to 1 pixel is defined, including a certain distance of H and V from the border of the pixels covering the tracked particle is defined. The algorithm effectively finds an arbitrary thickness of this rectangular frame. For each pixel that is used to create this frame, the intensity value is read, and the algebraic background average intensity (i.e., the Background Intensity, BI) is calculated. Within the next step of the tracking procedure, the intensity weight (IW) for each pixel surrounded by the defined frame is calculated as

$$\mathrm{IW} = \frac{\mathrm{PI}-\mathrm{BI}}{\mathrm{BPI}-\mathrm{BI}} \tag{1}$$

where PI is the pixel intensity in given location bordered by the rectangle frame used for calculation BI. As previously mentioned, a portion of the particle always partially occupies the area of the pixels around the base pixel, where the pixels intensity lies outside of the defined threshold range (see Fig. 7). To accurately calculate the particle size in the x and y directions, the effective diameter, and particle area, these pixels must also be considered. The largest of the values stored in the two vectors is considered to be the size of the particle in the x and y directions, respectively. An example of the described procedure used at the real particle is depicted in Fig. 7 (right).

An important parameter which can help in retrieving kinetic data of burned coal is the particle sphericity. This parameters helps in prediction movement of the particles, their vorticity and dispersion of the particles in real systems. The procedure used for calculating particle

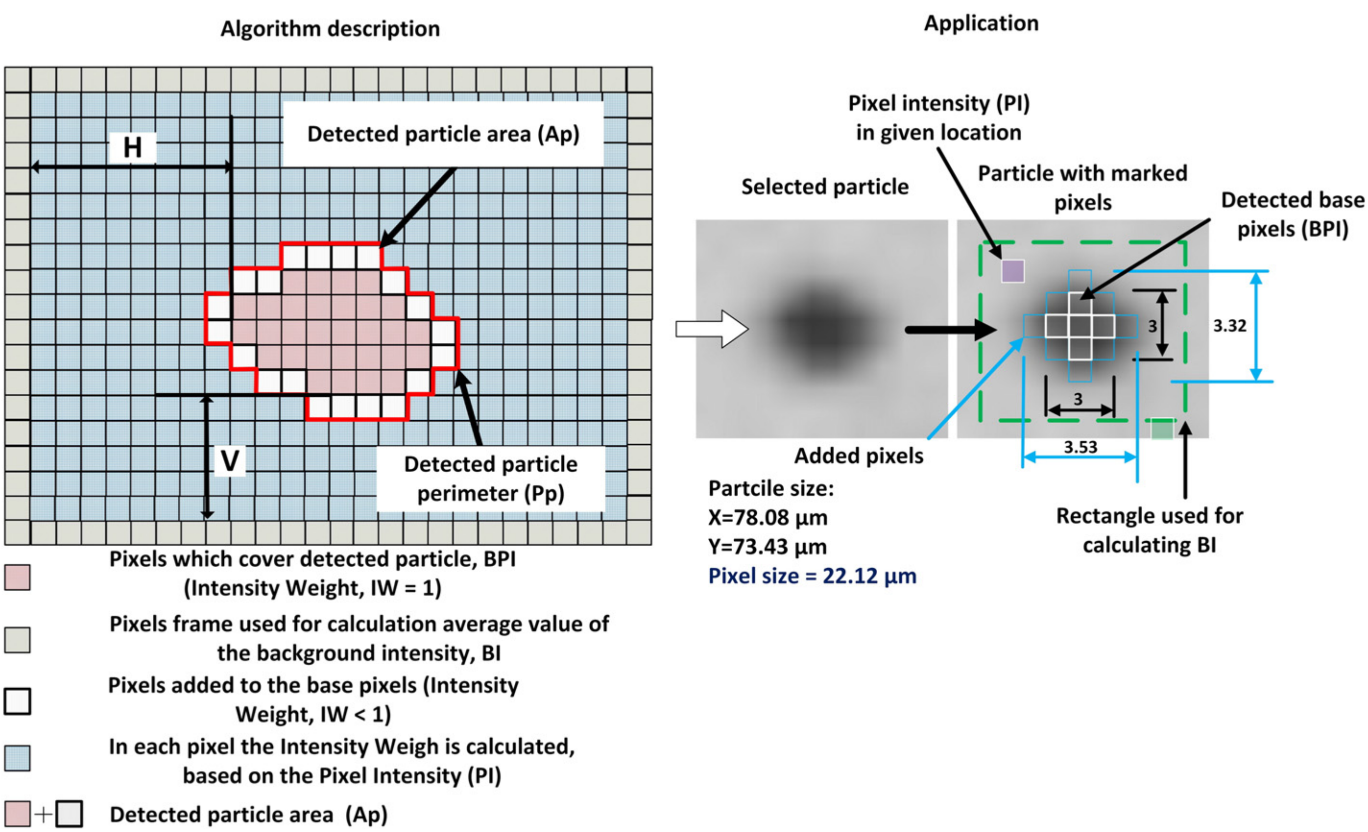

Fig. 7. Graphical illustration of the procedure used for detecting particle size and area (left) and their application for real particle (right).

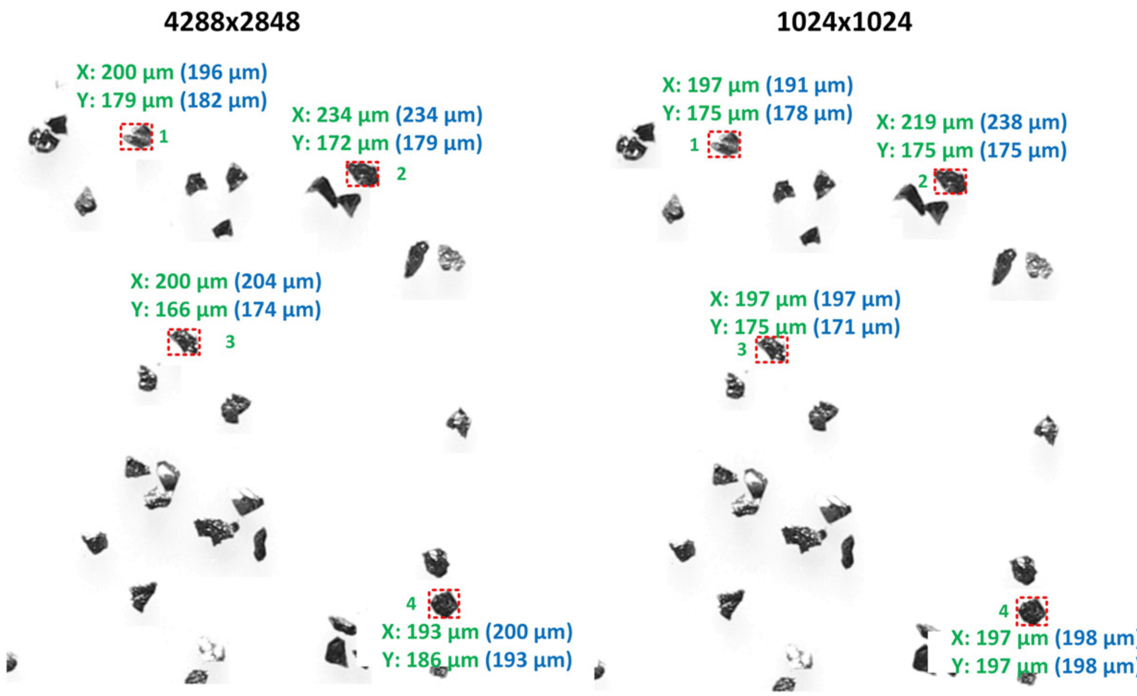

Fig. 8. Example of measured particle sizes based on manual detection and using computer algorithm.

sphericity, was implemented into the tracking procedure based on the algorithm used in commercial devices [36,37], where the particle sphericity is calculated based on the particle perimeter P_p and area A_p (see Fig. 7)

$$S = \frac{2\sqrt{A_p}}{P_p}. \tag{2}$$

5. Validation of the tracking algorithm

The method and algorithm presented in this study have been tested using a group of particles with particle sizes that have been manually checked using the optical method described in [38]. The validation procedure occurred as follows. First, the required particle size group was classified using a group of sieves, while the next step selected particles that were scattered on a flat surface covered by the glue. Such a prepared sample was photographed using high resolution camera (1 mm was covered by 145 pixels) and using installed on experimental rig CMOS camera (1 mm was covered by 44 pixels). Photographed samples next were analyzed manually and using a developed computer algorithm. In Fig. 8 the example of analyzed particle using both mentioned methods is illustrated. The particle sizes were calculated twice using both recorded images. The particle dimensions placed in round brackets corresponds to particle size calculated using computer algorithm. The differences between detected particle sizes for high and low resolution images based on manual measurement and using computer algorithm are illustrated in Fig. 9. It can be seen that differences in calculated particles sizes in x and y directions are very small in case of using computer algorithm, which ensure that the tracking procedure works with acceptable accuracy.

The collected size distribution using manual detection, computer algorithm and computer algorithm for carried particles in experimental rig is shown in Fig. 10. The particle size distribution diagram detected within the experimental rig was found to be shifted to smaller particle sizes; this situation was likely caused by the behaviour of particles carried by the gases, in which particles can spin from frame to frame.

To ensure the appropriate definition of the threshold range during the measurement of the particle size distribution in the oxidizing gas, it must be defined based on investigations using a given particle-size group in an inert gas. The defined threshold range can then be used to measure changes in particle size during combustion. The influence of

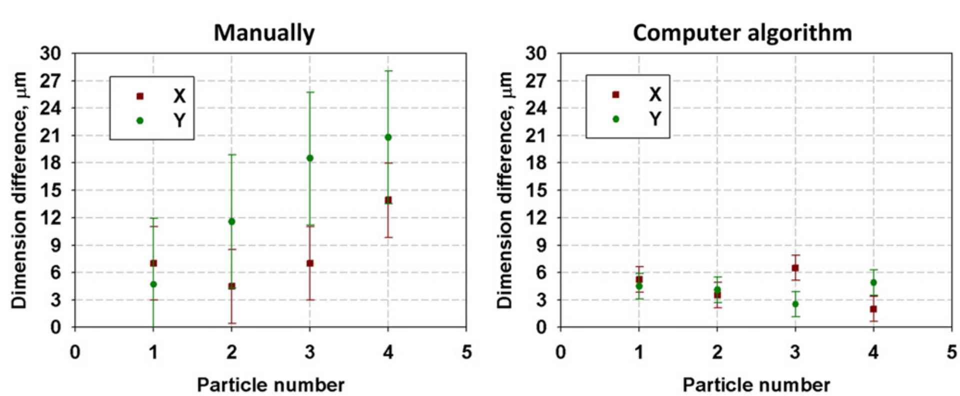

Fig. 9. Particle size differences obtained from manual algorithm and using the computer algorithm.

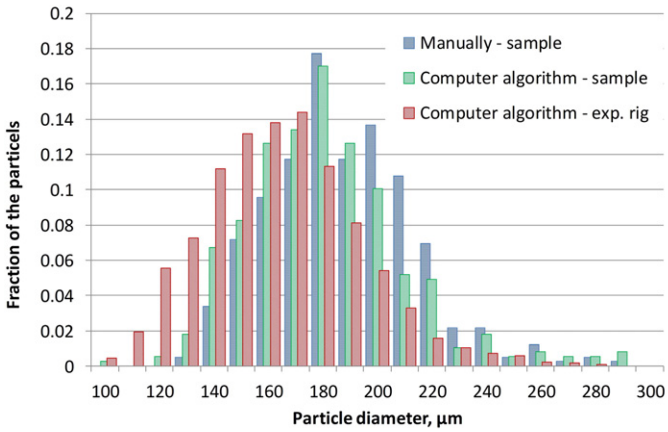

Fig. 10. Comparison of the manual method against the computer algorithm.

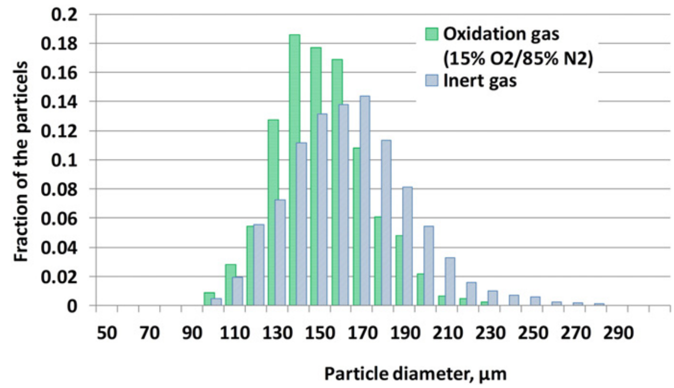

Fig. 12. The measured particle size distribution tracked in inert and oxidation gas atmospheres.

the threshold range on the predicted particles size distribution function is shown in Fig. 11.

Fig. 12 shows the measured particle size distribution of the particles tracked in the inert and oxidizing gases (15% of O_2 and 85% of N_2). It is shown that the particle size distribution diagram is shifted to smaller particle sizes due to the partial burning of the char; this increases the fraction of smaller particles observed. This effect is less noticeable for smaller particles because they can contain a smaller fraction of combustible material. The effect of particle mass loss can also be seen on the recorded particle trajectories in Fig. 13. The burned particles exhibit bent trajectories due to their mass loss compared to unburned particles or particles which consist only ash. The proposed technique can also yield information on the effect of non-spherical shape of a particle. The particle rotation effect is shown in Fig. 14, where the changes in particle sphericity within the subsequent frames for four arbitrary selected particles is shown. The particle sphericity has direct influence on the particle behaviour. When particles are not perfectly round it can rotes around the particle centre of gravity causing particle variation about the mean value. In real operating condition this parameter is very important because, it influences the mixing of the particle with oxidizing gases (burners construction) and strongly depends on the fluid shear stresses in vicinity to the particle.

Moreover, to check the tracking algorithm the results were tested against measured data collected using the commercial device [36] under cold flow conditions. In both tests the same coal sample was used. The measured distribution functions, using both devices are shown in Fig. 15. The measured, average particle sphericity using commercial device was 0.735 where using the in-house algorithm it was equal to 0.741.

Aside from the tracking procedure the rig allows one to capture the moment of particle ignition. Some example of particle ignition process was depicted in Fig. 16. This feature can be used for determination rate of particle ignition and further used for observation the particle heating rate by a system for measuring particle temperature (not implemented yet). Moreover, the knowledge about ignition time is helpful for retrieving kinetic data as this time determines the moments when the inverse procedure should start.

6. Formulation of the inverse problem

The inverse problem can be described as an iterative optimization loop within which, the sought for parameters (decision variables) are modified, so as to produce minimum discrepancy between the model and the measurements. The model equations, also known as the direct problem are solved at each step of the iterative loop. In order to obtain the particle trajectories, i.e. the functions $x_p(t)$ and $y_p(t)$ a force balance is formulated, where t is time and x_p and y_p are the horizontal and vertical positions of the particle, respectively. The functions $x_p(t)$ and $y_p(t)$ can be calculated by solving

$$\frac{dx_p}{dt} = u_p \tag{3}$$

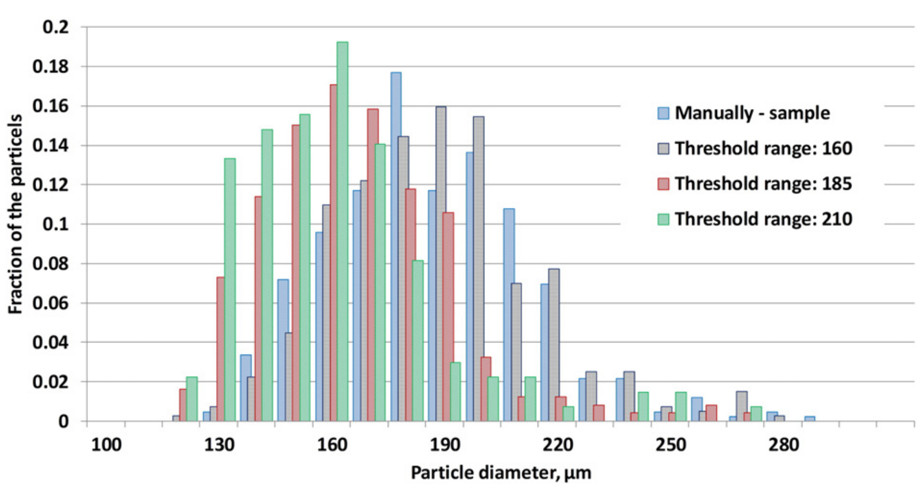

Fig. 11. Influence of defined threshold range on measured particle size distribution.

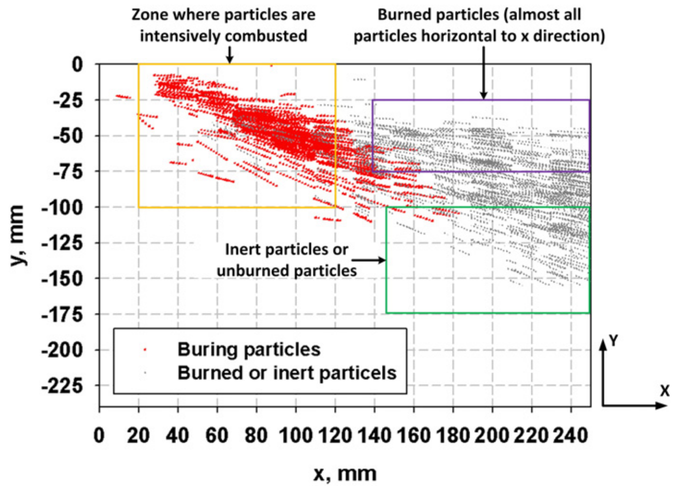

Fig. 13. Recorded particle trajectories.

$$\frac{dy_p}{dt} = v_p \tag{4}$$

The velocities u_p and v_p can be obtained from the force balances in x and y direction, which are written as follows [39,40]

$$\frac{du_p}{dt} = \frac{18\mu}{\rho_p d_p^2} C_d \frac{\mathrm{Re}_p}{24}(u - u_p) \tag{5}$$

$$\frac{dv_p}{dt} = \frac{18\mu}{\rho_p d_p^2} C_d \frac{\mathrm{Re}_p}{24}(v - v_p) + \frac{g\left(\rho_p - \rho\right)}{\rho_p} \tag{6}$$

where ρ and μ are the density and dynamic viscosity of the carrier gas, ρ_p and d_p are particle density and diameter, C_d is the drag coefficient, u and v are gas velocities in x and y direction, g is the gravitational

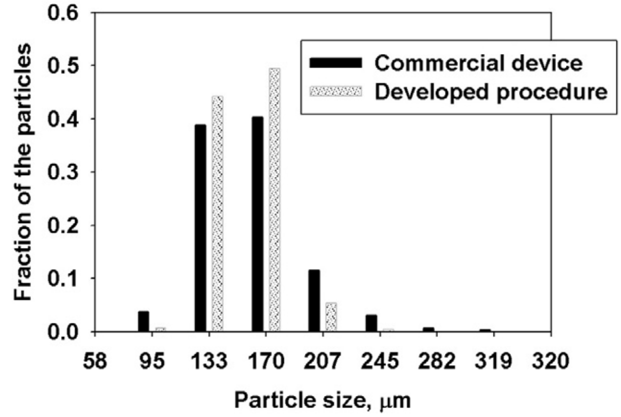

Fig. 15. Particle size distribution function measured using commercial device and developed procedure for tracking combusting particles.

acceleration and Re_p is particle's Reynolds number defined as

$$\mathrm{Re}_p = \frac{\rho d_p u_s}{\mu} \tag{7}$$

where u_s is the relative velocity of the fluid with respect to particle velocity (either $|u - u_p|$ or $|v - v_p|$). It is assumed that the particles are spherical and the drag coefficient is determined using the correlation by Morsi and Alexander [41]. The vertical gas velocity v is assumed to be 0 at all times. The horizontal gas velocity profile $u(y)$ is determined from a CFD simulation of the flow in the reactor performed for the same conditions as in the experiment. Furthermore, at the current stage of the work, it is assumed that the rate of change of particle density due to reaction is given by

$$\frac{d\rho_p}{dt} = -\frac{6R_c}{d_p} \tag{8}$$

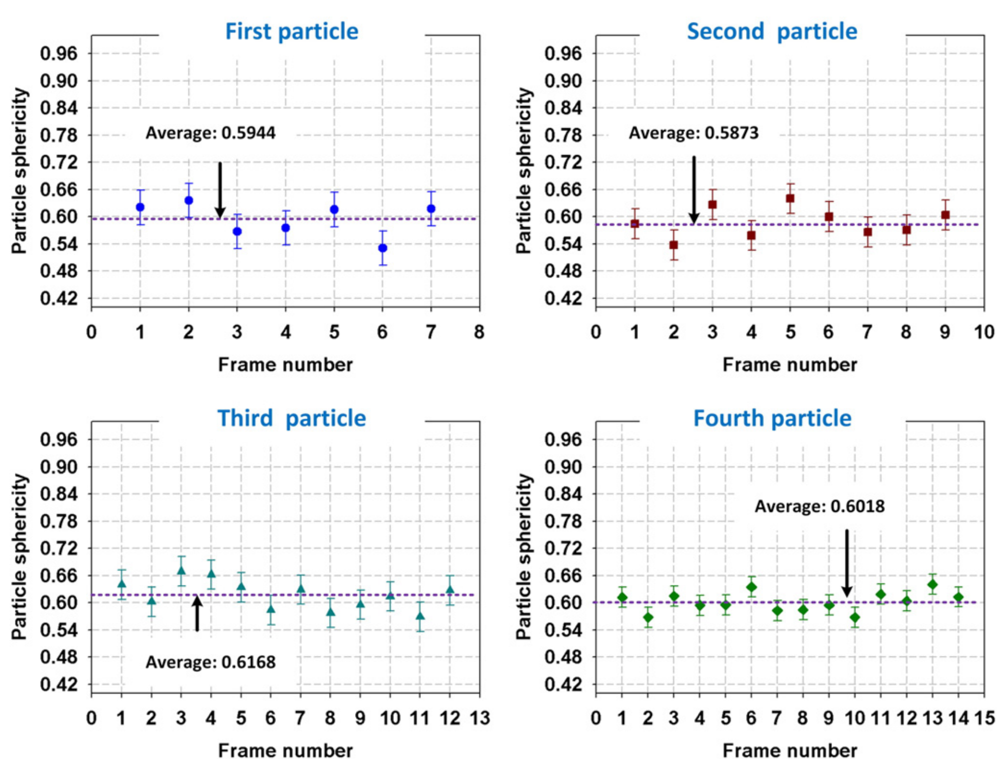

Fig. 14. Changes in the particle sphericity in subsequent frames for four selected particles.

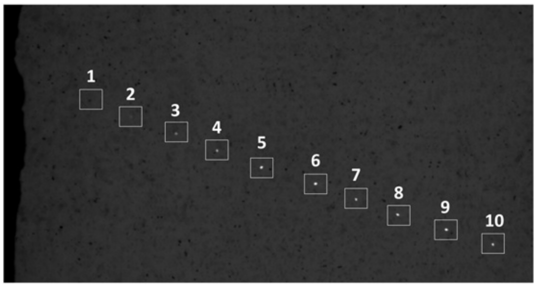

Fig. 16. Tracking particle ignition process.

Table 1
As-received ultimate and proximate coal composition used in experiments.

Prox., %		Ulti., %	
Ash	12.3	C	58.21
Water	11.0	H	4.00
Vol	30.43	S	1.52
Char	45.9	N	0.91
		O	12.06

where R_c is the reaction rate constant to be determined. Set of ordinary differential Eqs. (3)–(8) is solved using an explicit Runge-Kutta (4,5) method, the Dormand-Prince pair, implemented in MATLAB [42] (ode45 solver) with the following initial conditions

$$\begin{cases} x_p(0) = 0 \\ y_p(0) = 0 \\ u_p(0) = 0 \\ v_p(0) = 0 \\ \rho_p(0) = \rho_{p,0} \end{cases} \tag{9}$$

The reaction rate constant R_c entering Eq. (8) can be determined by solving the following minimization problem

$$\min_{R_c} F = \min_{R_c} \sum_{i=1}^{N} w_i \left[\left(x_{p,i}(R_c) - \overline{x}_{p,i} \right)^2 + \left(y_{p,i}(R_c) - \overline{y}_{p,i} \right)^2 \right] \tag{10}$$

where the F defines the objective function, $x_{p,i}$ and $y_{p,i}$ are the experimentally determined mean particle positions at N points and w_i is the weight calculated as a ratio of the number of trajectories used to determine the mean position at point i to the total number of recorded trajectories. The minimization is accomplished using the Levenberg-Marquardt method [43,44] implemented in MATLAB [42].

6.1. Retrieving coal kinetic data

The methodology presented in this work was tested using bituminous coal (Table 1). The experiments were carried out for different oxidation conditions. Initially, the particles were tracked in air at two different temperatures $T = 850\ ^\circ C$, $T = 950\ ^\circ C$. The fitted particles trajectories to the mean experimental data for considered cases are shown in Fig. 17, where also the retrieved combustion rates constants are presented.

Within next test, the burning particles were tracked for four O_2/CO_2 mixtures ($O_2 = [9,12,15,18]\%$ vol) at gas temperature $T = 1000\ ^\circ C$. The example of fitted trajectory to the experimental data for 18%O_2/82%CO_2 is depicted in Fig. 18. It can be observed that after a certain time, the predicted trajectory becomes a straight line which corresponds to a point where all carbon was consumed and the particle becomes non-reacting (ash), see Fig. 13. The retrieved reaction rate constants R_c for all the analyzed cases are presented in Fig. 19. As expected the reaction rate constant increases with increasing oxygen concentration and the increase is non-linear. More experimental tests, as well as their detailed analysis will be carried out in our further research to obtain results for other conditions and solid fuel chars.

7. Summary

Combined with a visualization system, the experimental rig used in this study has been successfully used for tracking particles under combustion conditions. The computer algorithm used to detect particle size has been validated against the simple manual method, showing good agreement. The proposed tracking procedure allows for the retrieval of kinetic data of the burned solid fuels under different combustion conditions. The described technique loses some accuracy by not considering the third dimension; thus, research that will improve the visualization system using an additional camera is planned to allow the observation of particles in three-dimensional space. The experimental rig developed in this study will be equipped with a system for measuring particle temperature during combustion processes. Further, presented method will be validated against data taken from experiments

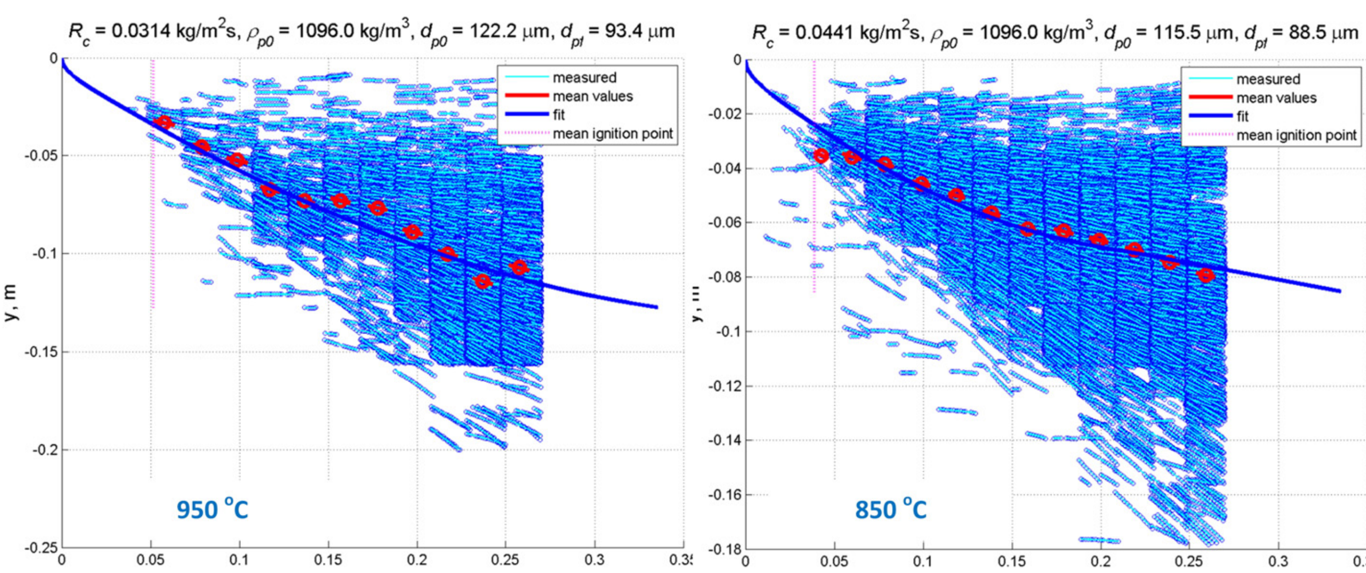

Fig. 17. Fitted trajectories to the experimental data carried out for air oxidation atmosphere.

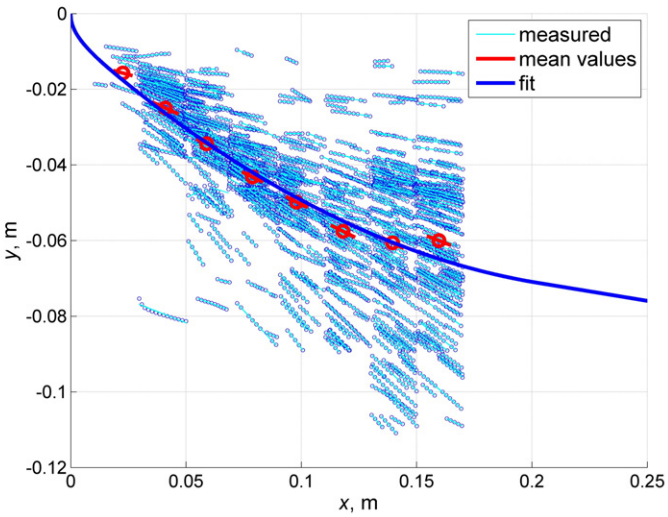

Fig. 18. Fitted trajectory to the experimental data.

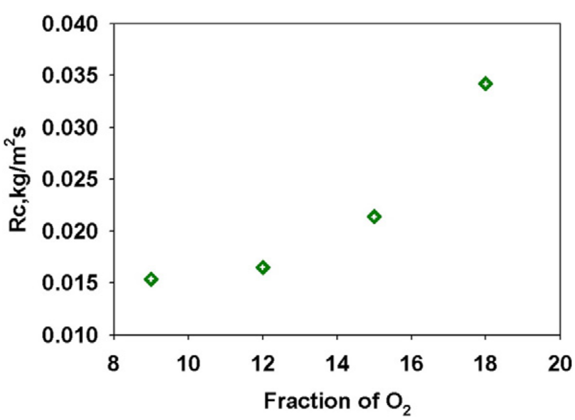

Fig. 19. Reaction rate constants determined for various O_2/CO_2 mixtures at 1000 °C.

carried out using DTF or TGA in specific combustion regime. Set of experimental work will be conducted for different coals, both hard and lignite one. Within the next step retrieved combustion rates of selected coal will be used as the input data to the numerical model used for simulating coal combustion process within industrial scale PC boilers.

Acknowledgements

The research leading to these results has received funding from the Polish-Norwegian Research Programme operated by the National Centre for Research and Development under the Norwegian Financial Mechanism 2009-2014 in the frame of Project Contract No Pol-Nor/232738/101/2014.

References

[1] M. Bugge, O. Skreiberg, N.E. Haugen, P. Carlsson, E. Houshfar, T. Lovas, Numerical simulations of staged biomass grate fired combustion with an emphasis on NOx emission, Energy Procedia 75 (2015) 156–161.
[2] F. Lockwood, S. Rizvi, N. Shah, Comparative predictive experience of coal firing, Proc. Inst. Mech. Eng. C J. Mech. Eng. Sci. 200 (23) (1986) 79–87.
[3] B. Higgins, L. Yan, H. Gadalla, J. Meier, T. Fareid, G. Liu, M. Milewicz, A. Repczynski, M. Ryding, W. Blasiak, Biomass co-firing retrofit with ROFA for NOx reduction, Pol. J. Environ. Study 19 (6) (2010) 1185–1197.
[4] W. Adamczy, P. Kozolub, G. Wecel, A. Ryfa, Simulations of the PC boiler equipped with complex swirling burners, Int. J. Numer. Methods Heat Fluid Flow 25 (4) (2014) 845–860.
[5] L. Chen, S. Zheng, A. Ghoniem, Oxy-fuel combustion of pulverized coal: characterization, fundamentals, stabilization and CFD modeling, Prog. Energy Combust. Sci. 38 (2012) 156–214.
[6] O. Authier, E. Thunin, P. Plion, C. Schonnenbeck, G. Leyssens, J.-F. Brilhac, L. Porcheron, Kinetic study of pulverized coal devolatilization for boiler CFB modeling, Fuel 122 (2014) 254–260.
[7] R.E. Mitchell, Experimentally determined overall burning rates of coal chars, Combust. Sci. Technol. 53 (2–3) (1987) 165–186.
[8] T. Joutsenoja, J. Saastamoinen, M. Aho, R. Hernberg, Effects of pressure and oxygen concentration on the combustion of different coals, Energy Fuel 13 (1) (1999) 130–145.
[9] R.H. Hurt, R.E. Mitchell, Unified high-temperature char combustion kinetics for a suite of coals of various rank, Symp. Combust. 24 (1) (1992) 1243–1250.
[10] T. Wall, Y. Liu, C. Spero, L. Elliott, S. Khare, R. Rathnam, F. Zeenathal, B. Moghtaderi, B. Buhre, C. Sheng, R. Gupta, T. Yamada, K. Makino, J. Yu, An overview on oxyfuel coal combustion - state of the art research and technology development, Chem. Eng. Res. Des. 87 (2009) 1003–1016.
[11] M. Baum, P. Street, Predicting the combustion behavior of coal particles, Combust. Sci. Technol. 3 (5) (1971) 231–243.
[12] L. Alvarez, M. Gharebaghi, M. Pourkashanian, A. Williams, J. Riaza, C. Pevida, J. Pis, F. Rubiera, CFD modelling of oxy-coal combustion in an entrained flow reactor, Fuel Process. Technol. 92 (2011) 1489–1497.
[13] J. Stenberg, W. Frederick, S. Bostrom, R. Hernberg, M. Hupa, Pyrometric temperature measurement method and apparatus for measuring particle temperatures in hot furnaces: application to reacting black liquor, Rev. Sci. Instrum. 6 (5) (1996) 1976–1984.
[14] T. Joutsenoha, P. Heino, R. Hernberg, B. Bonn, Pyrometric temperature and size measurements of burning coal particles in a fluidized bed combustion reactor, Combust. Flame 118 (5) (1999) 707–717.
[15] P. Edge, M. Gharebaghi, R. Irons, R. Porter, R. Porter, M. Pourkashanian, D. Smith, P. Stephenson, A. Williams, Combustion modelling opportunities and challenges for oxy-coal carbon capture technology, Chem. Eng. Res. Des. 89 (2011) 1470–1493.
[16] M. Cloke, E. Lester, A. Thompson, Combustion characteristics of coals using a drop-tube furnace, Fuel 81 (6) (2002) 727–735.
[17] H. Kruczek, M. Ostrycharczyk, M. Czerep, M. Baranowski, J. Zgóra, Examinations of the process of hard coal and biomass blend combustion in OEA (oxygen enriched atmosphere), Energy 92 (2015) 40–46.
[18] W. Chen, J. Wu, An evaluation on rice husks and pulverized coal blends using a drop tube furnace and a thermogravimetric analyzer for application to a blast furnace, Energy 34 (2009) 1458–1466.
[19] D. Vamvuka, E. Woodburn, A model of the combustion of a single small coal particle using kinetic parameters based on thermogravimetric analysis, Int. J. Energy Res. 22 (1998) 657–670.
[20] W. Wanga, A. Lawal, P. Stephenson, J. Sidders, C. Ramshaw, Post-combustion CO_2 capture with chemical absorption: a state-of-the-art review, Chem. Eng. Res. Des. 89 (2011) 1609–1624.
[21] G. Lu, D. Do, A kinetic model for coal reject pyrolysis at low heating rates, Fuel Process. Technol. 28 (1) (1991) 36–48.
[22] A. Sarwar, M. Khan, K. Fizza, Kinetic studies of pyrolysis and combustion of Thar coal by thermogravimetry and chemometric data analysis, J. Therm. Anal. Calorim. 7 (2011) 109.
[23] American Society for Testing and Materials, http://www.astm.org.
[24] M. Field, Rate of combustion of size-graded fractions of char from a low rank coal between 1200 K - 2000 K, Combust Flame 13 (1969) 237–252.
[25] Dantec Dynamics, On-line: www.dantecdynamics.com.
[26] R. Khatami, C. Stivers, K. Joshi, Y. Levendis, A. Sarofim, Combustion behavior of single particles from three different coal ranks and from sugar cane bagasse in O_2/N_2 and O_2/CO_2 atmospheres, Combust. Flame 159 (2012) 1253–1271.
[27] Y.A. Levendis, K. Joshi, R. Khatami, A.F. Sarofim, Combustion behavior in air of single particles from three different coal ranks and from sugarcane bagasse, Combust. Flame 158 (3) (2011) 452–465.
[28] M. Cloke, T. Wu, R. Barranco, E. Lester, Char characterization and its applications in a coal burnout model, Fuel 82 (2003) 1989–2000.
[29] J. Bibrzycki, PhD Thesis: Investigations of Coal Particle Combustion and Gasification, Institute of Thermal Technology, Silesian University of Technology, Poland.
[30] J. Bibrzycki, M. Mancini, A. Szlêk, R. Weber, A char combustion sub-model for CFD-predictions of fluidized bed combustion - experiments and mathematical modeling, Combust. Flame 163 (2016) 188–201.
[31] R. Hernberg, J. Stenberg, Simultaneous in situ measurement of temperature and size of burning char particles in a fluidized bed furnace by means of fiberoptic pyrometry, Fuel 95 (1–2) (1993) 191–205.
[32] T.M. Linjewilea, A.S. Hulla, P.K. Agarwal, Optical probe measurements of the temperature of burning particles in fluidized beds, Fuel 73 (12) (1994) 1880–1888.
[33] M. Ozisik, H. Orlande, Inverse Heat Transfer, Fundamentals and Applications, Taylor and Francis, New York, 2000.
[34] ANSYS, Inc., ANSYS FluentOn-line, www.ansys.com.
[35] C. Igathinathane, S. Melin, S. Sokhansanj, X. Bi, C. Lim, L. Pordesimo, E. Columbus, Machine vision based particle size and size distribution determination of airborne dust particles of wood and bark pellets, Powder Technol. 196 (2009) 202–212.
[36] G. Crolly, FRITSCHOn-line www.fritsch.de.
[37] P.P.S. Systems, On-line www.pssnicomp.com (8203 Kristel Circle, Port Richey, FL 34668).
[38] M. Rhodes, Introduction to Particle Technology, second ed. John Wiley & Sons, Ltd, 2008.
[39] P. Sreekanth, M. Syamlal, T. O'Brien, Computational gas-solids flows and reacting systems: theory, methods and practice, Engineering Science Reference, IGI Global, 2012 (ISBN 978-1-61520-651-2).

[40] C. Crowe, J. Schwarzkopf, M. Sommerfeld, Y. Tsuji, Multiphase Flows with Droplets and Particles, Taylor & Francis Group, 2012.
[41] S. Morsi, A. Alexander, An investigation of particle trajectories in two-phase flow systems, J. Fluid Mech. 55 (2) (1972) 193–208.
[42] MATLAB, Version 7.9.0.529 (R2009b), The MathWorks Inc., Natick, Massachusetts, 2009.
[43] K. Levenberg, A method for the solution of certain problems in least squares, Quart. Appl. Math. 2 (1944) 164–168.
[44] D. Marquardt, An algorithm for least-squares estimation of nonlinear parameters, SIAM J. Appl. Math. 11 (1963) 431–441.